Article type: *Original article*

Article title: On-board condition monitoring of rail axle bearings using vibrations.

Authors: Ilaria Corni[1], Nicola Symonds[1], Adam Wasenczuk[2] and David Vincent[2]

[1] nC[2], Faculty of Engineering and the Environment, University of Southampton, UK

[2] Perpetuum Ltd, Southampton, UK

Corresponding author: Ilaria Corni, nC[2], Faculty of Engineering and the Environment, University of Southampton, University Road, Southampton, Hampshire, SO17 1 BJ, UK. Email: i.corni@soton.ac.uk

Abstract

Premature failure of rail axle bearings generates a significant increase in train operating costs and can also affect train safety. In order to solve this problem a commercial on-board condition monitoring system has been fitted on numerous passenger trains, providing the operator with real-time information on bearing health. This new technology detects bearing damage effectively and promptly. The project of which this paper is a part aims to determine a relationship between vibrations and bearing damage. Filtering tools have been developed to parameterise extra vibrations due to bearing damage, and to compare vibrations produced by different bearings. Bearings, which failed in-service, have been analysed with surface profilometry, to quantify the damage. This paper highlights a requirement for a better understanding of the damage mechanisms involved in bearing failure and a more detailed characterization of the damage.

1. Introduction

Bearing failure can cause the breakdown of equipment, decrease its efficiency or even reduce safety with risks to life [1-3]; ensuring good condition is fundamental for train safety and this can be achieved using condition monitoring. Axle bearings are key elements in the integrity of railway wheel sets. The most common failure in rail axle bearings is due to rolling contact fatigue (RCF) of the outer ring [4, 5]. Sub-surface networks of cracks grow in the rolling direction by shear stresses and then deviate towards the surface causing 'macropits' [6-9]. The degradation is described in detail by El-Thalji and Jantunen [10]; they summarize the stages, the mechanism involved and the factors influencing each stage, how the degradation evolves from one stage to the next and how the surface changes during the life of the bearing. Because of this failure mechanism, bearings are considered "lifed" components and are regularly inspected for failure.

The degradation of rail axle bearings occurs with an increase in noise and vibration, followed by an increase in temperature [11]. For many years, the increase in temperature has been detected by trackside Hot Axle Box Detectors (HABDs); when the temperature rises, the train has to be stopped immediately producing disruption to passengers and railway traffic.

For this reason, research has been carried out to identify precursors to run-away thermal failure, using acoustic emissions and vibrations. Acoustic monitors utilise the frequency of the sound to detect the damaged component (e.g. damaged bearing, noises from flanging, wheel flat, gearbox noises). Entezami *et al.* [12] present

studies in which recording equipment and algorithms able to detect early stage bearing failures were developed in the laboratory; this technology was then applied to a real train showing great potential. In a similar study, they [13] measured using track-side equipment high-frequency acoustic emissions from freight rolling stock fitted with artificially damaged bearings and analysed these data using time spectral kurtosis. This methodology showed the capability to distinguish the noise generated by damaged rail axle bearings from other noise produced by different sources, e.g. wheel-track interaction, braking and speed variation. The same group also developed an on-board condition monitoring system consisting of high-frequency acoustic emission sensors and accelerometers installed on the axle-bearing housing of freight wagons. They demonstrated by integrating acoustic emission and vibrations data that wheel and axle-bearing defects with diverse levels of severity can be successfully detected [14, 15] and also, by applying envelope analysis to the acoustic emission signals, they could detect and evaluate the type of damage in the bearing [16]. Tsukahara *et al*. [11] compare the capability of two different Acoustic Bearing Detectors (ABD) (RailBAM and unknown) to identify eight faulty bearings fitted on a French TGV; after 57 runs at speed between 15 and 130 km/h both ABDs located correctly seven bearings out of eight. In the USA, axle bearings are monitored employing TTCI Trackside Acoustic Detection System (TADS®) that identifies defects before overheating [17].

Limited research has been reported on vibration condition monitoring of rail axle bearings. The SKF Multilog online system [18] consists of several modular sensors which monitor and transmit many bogie operating conditions (temperature and vibrations are measured for bearings). The SKF Axletronic sensor solution [19] measures vibrations, temperature, direction and speed and it can be distributed around the rail-axle bearing or in its front cover and it could be fitted on new railway vehicles or existing rolling stock. Deutsche Bahn Systemtechnik has developed an on-board bogie diagnostic system consisting of two units: the bogie instrumentation (noise and vibration sensors), linked by cables to the diagnostic unit under the passenger's seat. This technology can effectively detect early bearing damage [20]. Bellaj *et al*. [21] compare results from track-side ABD and on-board vibration measurements for a high speed TGV on which eight faulty bearings were fitted. The on-board system showed increased vibration for damaged bearings and successfully identified faulty bearings for speed higher than 60 km/h. The track-side detector recognized 75% of failed bearings using multiple runs and speed higher than 60 km/h. More recently, the MAXBE project [22] developed a synchronized on-board and trackside system consisting of strain gauges, high frequency accelerometers, temperature and acoustic emission sensors that collect values into an integrated platform. This system showed the capability to detect early stage axle bearing failures and to help determining strategies for condition-based maintenance of axle bearings.

The present paper presents an initial study to correlate vibration data with bearing damage. Vibration data are measured using a commercial condition monitoring system fitted to Southeastern operated rolling stock, which monitors vibrations in real-time, successfully detecting degrading rail-axle-bearings [4]. Faulty bearings detected with this methodology are sent to the University of Southampton where the damage is accurately quantified. The reason for this collaboration, and the choice of this particular sensor, is a rare opportunity to have access to the damaged bearings and their vibration history in-service. This represents a key factor for understanding the

bearing failure mechanism and the corresponding vibration signature. The objectives of the on-going research programme are:

1. to develop tools and techniques to compare the vibration data of damaged bearings removed from different trains.
2. to determine a relationship between the vibration data and the level of bearing damage.

This second aim is a larger task, beyond the scope of this paper, though five example bearings are here shown to demonstrate the methods and techniques being used to look at the possible relationships between vibration data and the extent of bearing damage.

2. Material and Methods

2.1 Sensors

The work is carried out in collaboration with Perpetuum Ltd., a Southampton (UK) based company, that has developed a novel on-board condition monitoring system for quantifying local vibrations in the train environment. The system consists of wireless sensor nodes (WSNs) that are bolted onto axle-bearing housings and are self-powered by vibrations using energy-harvesting technology. The WSN measures vibrations using a tri-axial accelerometer; the acceleration data are recorded for 4 seconds every 3 minutes. The sensor records 16,000 points per second on each axis (x is the vertical direction, y is the direction of travel and z is the direction of the axle); in 4 s of recording time 192,000 data points are recorded. These data points (raw data) are discarded after being employed to calculate: *rms X*, *rms Y*, *rms Z*, *peak X*, *peak Y, peak Z*, *bearing health index* (BHI) and *wheel health index* (WHI). These data combined with train number, wheel position, date and time, speed of the train, GPS location, direction of travel, and temperature are wirelessly sent to the Cloud and are available in real-time via a website. The train operating companies (TOCs) have real-time access to BHI and WHI values and use these data to identify bearing and wheel issues, respectively. BHI and WHI values are calculated by proprietary algorithms and as such have not been employed in this study.

2.2 The environment

This system is fitted on several networks in the UK and worldwide, but the current work concerns Southeastern trains, covering over 1,000 miles of tracks in the South-East of England. All the trains of the Southeastern Electrostar fleet (148 trains) are fitted with WSNs; these trains consist of 32 or 40 wheels for a total of 4,944 wheels that are continuously monitored during normal passenger service (1 WSN per wheel). GPS data returned by numerous WSNs have been plotted to determine the routes covered by these trains and the results have been overlaid to “Google map” (blue and orange lines shown in Figure 1).

Figure 1. Map of the South East of England. The track covered by Southeastern trains is indicated in blue and orange; the track Tonbridge to Ashford International is in orange.

2.3 Bearing type

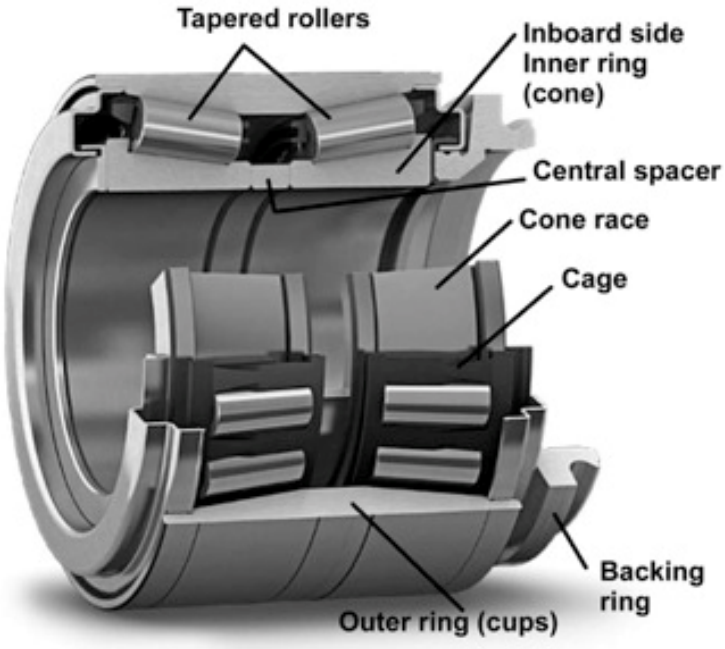

Figure 2. Schematic of a Compact Tapered Roller Bearing Unit (CTBU) (reprinted from Engineering Failure Analysis, 56, Symonds N, Corni I, Wood RJK, Wasenczuk A, Vincent D, Observing early stage rail axle bearing damage, 216-232, (2015), with permission from Elsevier).

The bearings studied in this work are Compact Tapered Roller Bearing Units (CTBUs) manufactured by SKF (see Figure 2) [23]. Each CTBU consists of:

- An outer ring with two symmetrical cup races;

- Two inner rings (cones) with 40 mm wide races;
- 23 tapered rollers rotating on each inner ring and kept in place by a polymeric cage.

Bearings with high BHI readings are removed by the operator and stripped at the Southeastern Ramsgate Maintenance depot. The bearings are then sent to the University of Southampton for further analysis. All the bearings that have been identified with high BHI values presented damage in at least one of the two cup races of the outer ring. The damage is always found in the top of the bearing relative to the bearing housing, which is the area subject to the maximum load.

2.4 Analysis of the damage

The surface profiles of the faulty outer rings were measured at Taylor Hobson Limited (Leicester, UK) using a Talyrond 595. The outer ring of the bearing was positioned on a spindle top and five traces of the whole rolling area were measured with high data density (72,000 points over 360°). The 0 mm trace was carried out outside the worn area of the race towards the centre of the outer ring and the others were 10 mm apart moving towards the outboard side of the race. The surface profile data were employed to calculate the area worn on each profile by multiplying *Pa* (arithmetic mean deviation from the original unworn profile) by the assessing length. These data could then be used to calculate the volume missing from the race of the outer ring by averaging the area missing in the 4 lines and multiplying it by 40 mm (width of the race).

3 Theory

3.1 Vibrations

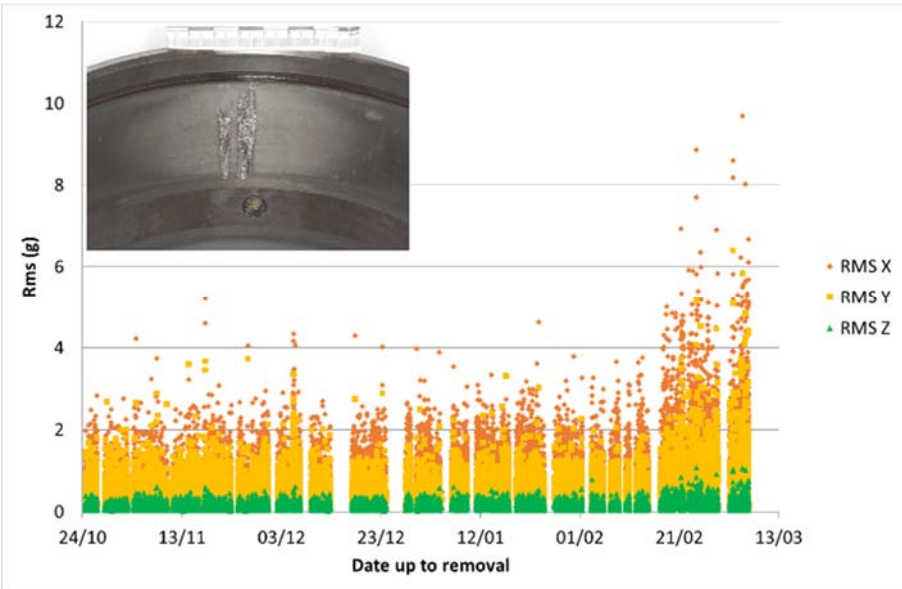

Figure 3. Rms vibrations in X, Y and Z measured by one sensor travelling on the Southeastern track (Figure 1) up to bearing removal, showing the increase in vibrations as the bearing degrades from a day in between 01/02 and 21/02. Insert showing RCF damage in one of the races of the outer ring of the removed bearing.

Twelve months of vibration data from numerous sensors from many healthy wheels and bearings travelling at different speeds in the Southeastern region of track (track highlighted in blue and orange in Figure 1) have been analysed in order to understand the sources of vibrations and how the vibrations change with time and GPS position. A general example of the vibrations of a "good" bearing is shown in the first part of the graph reported in Figure 3 (up to 01/02). Rms X and Y have generally values between 0 and 5 g and are much higher than rms Z values (generally below 0 and 0.5 g). This clearly demonstrates that the vibrations vary significantly from point to point, making a comparison quite challenging. This rapid variation is caused by the complexity of the bearing-wheel-axle-track system, which is affected by numerous factors (see Figure 4), such as:

1. train track (e.g. fish plates, track points, junctions between tracks),
2. wheel conditions,
3. bearing conditions,
4. loading over tuning,
5. train speed and
6. time (e.g. track conditions can change with time).

The vibrations change continuously but they are statistically reproducible over time and therefore they could be employed to map the railway line to identify changes in the infrastructure.

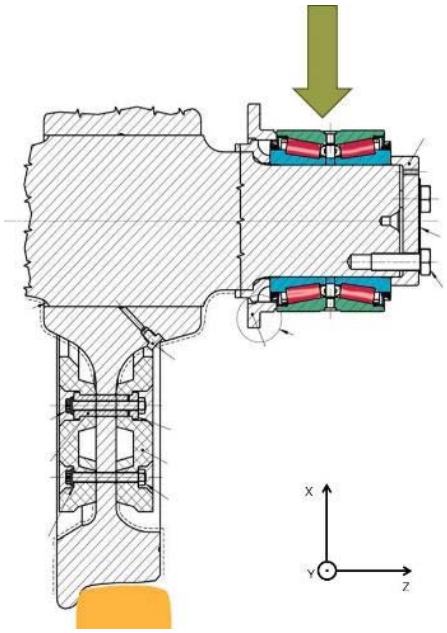

Figure 4 – Schematic of the system bearing-wheel-axle-track showing the bearing position with respect to the other components and the area of higher load.

3.2 Choice of one parameter

During this study, it has been observed that bearings with vibrations (*rms X*, *rms Y* and *rms Z*) higher than normal (as shown in the example reported in Figure 3) when inspected presented damage (e.g. rolling contact fatigue in one of the races of the outer ring). The mean value and the standard deviation for these three parameters

were calculated for healthy and damaged bearings; four examples, reported in Figure 5, clearly show that the vibrations in X, Y and Z for damaged bearings (D1 and D2) are almost double of those for healthy bearings (H1 and H2). Table 1 reports two examples where the mean and standard deviation were calculated for the period in which the vibrations were "normal" and "high" for the same bearing (as shown in the example in Figure 3). The information in Figure 5 and Table 1 clearly shows that any of these three parameters could be employed to detect degrading bearings. However, since the percentage increase of the vibration from "normal" to "high" clearly shows that rms X (vertical direction) has the largest change in value as the bearing degrades (Table 1), this parameter was chosen.

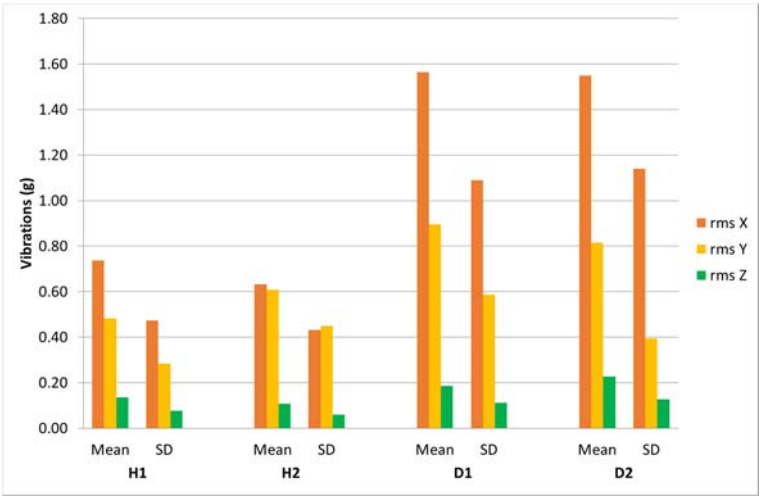

Figure 5. Mean vibration and standard deviation (SD) for rms X, Y and Z for four bearings, where H1 and H2 are examples of healthy bearings and D1 and D2 are examples of damaged bearings.

Table 1. Two examples of mean and standard deviation values for two damaged bearings calculated using the "normal" values and the "high" values and their percentage increase.

Examples		Normal value	High value	% increase
Bearing 1	X	0.83±0.52	1.56±1.09	89%
	Y	0.51±0.31	0.90±0.59	75%
	Z	0.13±0.07	0.19±0.11	45%
Bearing 2	X	1.14±0.68	1.55±1.14	36%
	Y	0.74±0.45	0.82±0.39	9%
	Z	0.18±0.09	0.23±0.13	25%

3.3 Filtering/reducing the data

In this study, in order to be able to compare the vibrations of bearings from different trains, the data have been 'decimated' to eliminate most of the factors affecting the vibrations and listed in Section 3.1. From the GPS data recorded, it is known that each train covers the whole Southeastern track (blue and orange in Figure 1) in a period between 2 and 6 weeks; therefore some of the factors affecting the vibrations can be eliminated by using data from only one part of the track. The straight part of track going *from Tonbridge to Ashford*

International (orange track in Figure 1) was chosen. The vibration data were 'filtered' using the GPS coordinates in the following intervals: latitude 51.1478 to 51.1927; longitude 0.2639 to 0.8591 and heading 86 to 116. This track was chosen because: being a predominantly straight track (approximately 40 km long) there are no extra vibrations due to curves (extra load on wheels during turning) and the data are easily plotted using latitude or longitude.

By comparing data from four trains (64 wheels) travelling from Tonbridge to Ashford International during the same 2-month period it has been demonstrated that: all the 16 wheels from the same side of the same train have the same vibration pattern (when they are in good health) independently from their position along the train and from the train type (results not shown here). The *effect of train track* and the *effect of time* were eliminated by comparing the data from the faulty bearing with the data of only the remaining "good" bearings on the same side of the same train, so that the contact rail-wheel is consistent and reproducible. This comparison between the damage bearing and the baseline can be carried out because the vibrations are the same for all the wheels independently from their position in the train. Therefore the vibrations of the "good" bearings (data from 15 WSNs) can be employed to produce the baseline vibrations typical for that train, track and period of time. There are now two aims:

- *Compare the vibrations of a damaged bearing with the baseline vibrations of the same train, journey and period of time (measured by 15 WSNs fitted on the same side of the same train).* Through this approach, it is possible to determine by how much and for how long the vibrations of the damaged bearing have been higher than the baseline vibrations. As the extra vibrations should be due to the damage in the bearing, these two parameters are fundamental to estimate the quantity of damage expected. The vibrations measured by the sensor go back to the baseline vibrations after bearing removal to make sure that there are no extra factors affecting the higher vibrations.
- *Compare the vibrations of different damaged bearings.* In order to be able to compare vibrations from different damaged bearings most of the factors affecting the vibrations need to be eliminated by filtering/reducing the data set. The only parameters affecting the filtered data are: *speed, wheel damage* and *bearing damage*. The *effect of wheel damage* is removed by confirming that the WHI values transmitted by the sensor are within the limits for healthy wheels. This ensures that the extra vibrations measured are not due to wheel damage. The effect of speed could be eliminated by using only one particular speed, but this approach was not implemented because it was found that it seriously decreased the number of data points available making comparison between different degrees of damage very difficult.

4 Results

The vibration data (Section 4.1) and the surface damage (Section 4.2) of five bearings removed from service from the same type of train (375900 series) are described in this section with the aim to find some parameters that could be employed to then compare the vibrations and the damage. In Section 3.3, it has been suggested that

the vibrations are independent from the train type but, in order to reduce the risk of this correlation, examples from only one type of train are employed.

4.1 Comparison of vibration data

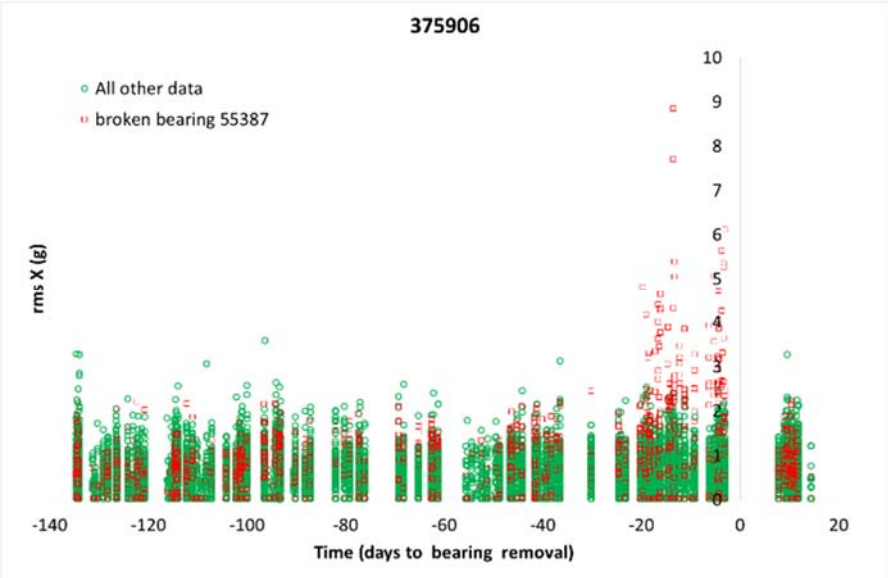

Figure 6. Example of vibrations in rms X for the damaged bearing in Figure 3 (in red) compared with its baseline (in green) from other bearings on the same side of the same train for the same journeys and the same period of time. Day 0 corresponds to bearing removal.

Table 2. Parameters describing the five bearings.

Bearing	A	B	C	D	E
Serial number	55387	55105	39913	90873	55552
Position in the train	MOS6	MOS3	DB3	DB8	DB4
Bearing fitted for (months)	55	56	50	56	56
Mileage (1,000 miles)	485	475	423	501	495
WSN fitted for (months)	4.5	3	9	4.5	4.5
Highest rms X value (g)	8.86	4.93	8.43	6.02	7.06
Last rms X value (g)	2.46	1.47	2.80	1.75	6.23
Days different from baseline	-30	-61	-94	-104	-22
Damage length (mm)	16	22	70	70	56
Volume loss (mm^3)	61	101	450	662	740

In this study, the vibration data have been analysed comparing the data of the failed bearing with the baseline vibrations of the other bearings on the same train covering the same track and subjected to the same speed profiles and loadings, as described in Section 3. This method identifies extra vibrations related to the damage.

Figure 6 shows an example of this process: the vibrations of the damaged bearing, reported in Figure 3, are compared with its baseline from other bearings on the same side of the same train. The data in Figure 6 are from track going only from Tonbridge to Ashford International; the data in Figure 3 were collected in the whole Southeastern region. By comparing these data it is clear that the filtered data (Figure 6) are still representative of the original trend measured across the Southestern region (Figure 3). After bearing removal, on day 0, the vibrations of the "damaged bearing" decreased and became very similar to the baseline, as expected. The vibrations of the other four bearings analysed in this paper compared with their baselines are summarised in Table 2.

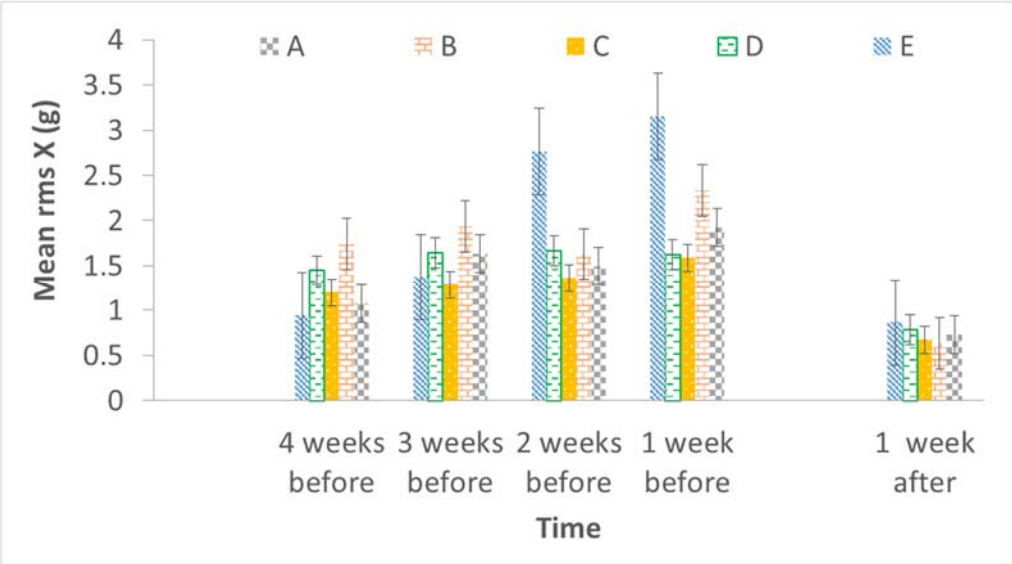

Figure 7. Mean rms X values recorded over the last 4 weeks of use before removal of each bearing and 1 week after fitting a new bearing. The values from bearing E recorded in the last two weeks are significantly higher than those for the other bearings.

For bearings E and A the vibrations are very similar to the respective baseline vibrations until 22 and 30 days before bearing removal when they rapidly increased to 7.06 and 8.86 g, respectively. The vibrations of bearings B and D started to behave differently from the baseline 61 and 104 days before bearing removal and they increased slowly and only up to 4.93 and 6.02 g, respectively. Bearing C had vibrations similar to the baseline up to 94 days before removal; the vibration data reached the maximum (8.43 g) 80 days before removal and then decreased to 4g upon bearing removal. The vibrations of all five WSNs /decreased considerably and went back to the value typical of the baseline after new bearings were fitted, further confirming that the extra vibrations measured were due only to bearing damage.

The highest value of vibration, the last vibration value and the number of days the vibrations have differed from the baseline (Table 2) could all be employed to compare vibrations and damage. In the last two weeks before removal, the mean values of rms X are 30 to 50% higher for bearing E compared to the other four bearings that show a similar level of vibration in comparison to each other.

Based only on the vibration parameter employed, the bearings could be ordered by decreasing severity in several ways:

- highest rms X value reached (Table 2): A, C, E, D and B;
- last rms X value reached (Table 2): E, C, A, D, B;
- days different from the baseline (Table 2): D, C, B, A and E;
- mean rms X values (Figure 7): E and B appear worse than A, C and D.

4.2 Characterization of the damage

Figure 8 shows images of the damage found in the outer rings of the five bearings removed from service after the increased level of vibrations described in Section 4.1. The damage observed in these bearings has clear signs of rolling contact fatigue [4, 6] and is similar to that reported in other studies of rail axle bearings [11, 18, 20]. Bearings E (Figure 8e) and D (Figure 8d) show 56 and 70 mm, respectively, of uniform circumferential damage. Bearings B (Figure 8b) and A (Figure 8a) show a smaller damage over only 22 mm and 16 mm, respectively; these damages are in two separate areas as if they have been initiated separately: one is as wide as the race and the other is smaller. Bearing C (Figure 8c) shows two damaged areas that are as wide as the race and connected only through a small area, and a separate very small damage. An example of the profile of one damaged area obtained using surface profilometry is shown in Figure 9 and the most important values used to quantify the damage for these bearings: damage length and volume worn, are listed in Table 2.

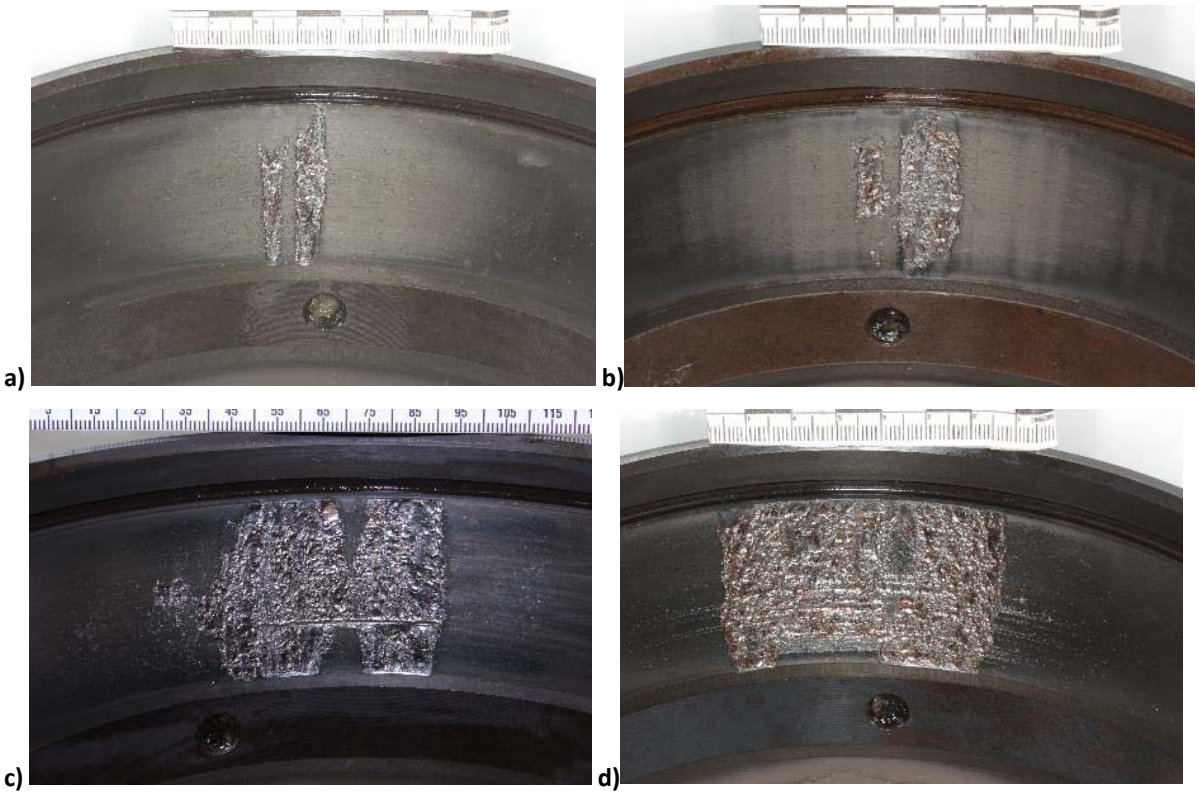

e) 

Figure 8 – Damages on the outer ring for the five bearing studied: (a) 55387, (b) 55105, (c) 39913, (d) 90873 and (e) 55552.

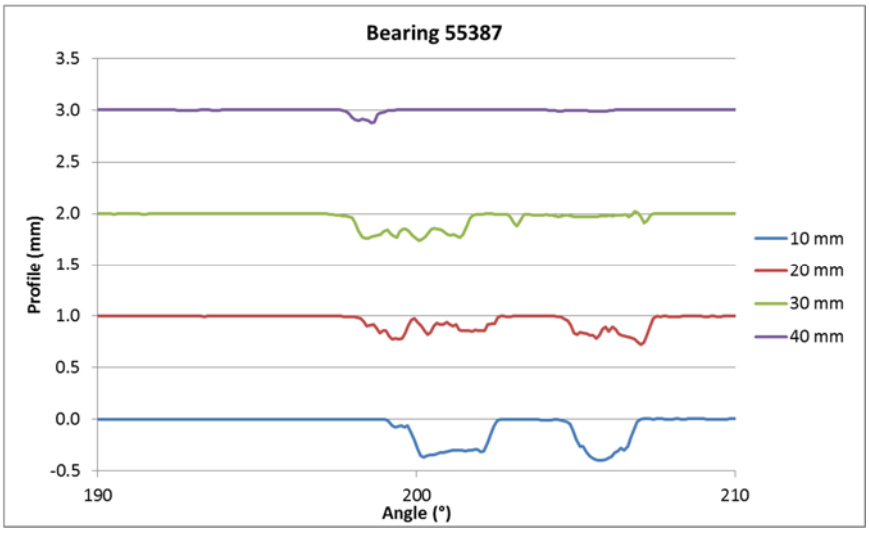

Figure 9. Example of surface profile of bearing 55387.

From a damage point of view (Figure 8) bearings A and B display significantly less damage than the other three bearings (C, D and E), considering the damage length, the volume missing and the area worn. Moreover, bearings D and E have deeper damage and a higher volume missing than bearing C (Table 2).

5 Discussion

The commercial system produced by Perpetuum Ltd identifies damaged bearings through 'BHI' values calculated with their proprietary algorithm. In this study, the raw data have been re-analysed using a different approach. The data have been filtered using data recorded from the same part of the track (Tonbridge to Ashford International), and therefore subjected to the same speed profiles and loadings to eliminate as many variables and influences as possible. Knowing that:

1. all the sensors, independently from wheel position on the train, are producing the same vibration signature (if there is no bearing or wheel damage);
2. The extra vibrations produced by a faulty bearing are due to the damage in the bearing itself.

the vibrations of different damaged bearings can be compared like-for-like and linked with their corresponding damage.

The rankings presented in Sections 4.1 and 4.2 clearly demonstrate that there is not a readily available relationship between vibration and damage length or volume worn.

It has been observed in Section 4.1 that the vibrations of different bearings grow with different slopes and at different speeds, indicating that there are different parameters affecting the damage growth and consequently the vibrations measured. The following variables could influence the vibration/damage correlation:

- Isolated loading (overload) events that have not been captured by the WSN or have been filtered out.
- History of the bearing before the WSN was fitted.
- Metallurgical differences between the bearings. For example, a bearing with a large sub-surface flaw, like the one described in [4], may present a unique damage/vibration pattern; the RCF cracks may all grow sub-surface producing almost no measurable vibrations until a large macropit is released generating suddenly very high vibrations. Using the time that the vibrations differed from the baseline as a parameter to compare bearings assumes that RCF progresses at the same speed and since this is not true, this parameter might not be the best parameter for this comparison.
- The physical growth of the damage (e.g. the shape, the depth and the number of RCF macropits) could influence the vibration signature as could also the subsequent smoothing of the fracture surface.

Therefore, it is proposed that further research needs to focus on a more detailed characterization of the damage, a better understanding of the mechanisms initiating bearing failure, the propagation of the damage and the kind of damage that is generated by different failures. This knowledge will help in understanding the complex relationship between vibration and damage. More examples of damage and vibrations are needed in order to achieve a more complete understanding of this complex relationship.

Conclusions

1. Limiting this study to *rms X* and filtering the data to those collected while travelling on a length of straight track allows comparison of the vibrations of in-situ damaged bearings.
2. An effective parameterisation methodology to present vibration data has been developed.
3. Determining the effect that the damage plays on the vibrations requires more detailed characterization and parameterisation of the damage.

Acknowledgements

The authors gratefully acknowledge Southeastern and Perpetuum staff for their assistance during the work.

Funding

This work was supported by the Engineering and Physical Sciences Research Council (EPSRC) [Impact Acceleration Account] and by WARNTRAK 672265 (Horizon 2020-SMEINST-2-2014).

References

1 - Gao RX, Jin Y, Warrington RO, Microcomputer-Based Real-Time Bearing Monitor, IEEE Transactions on instrumentation and measurement 1994; 43: 216-219.
2 - Lei Y, Lin J, He Z, Zuo MJ, A review on empirical mode decomposition in fault diagnosis of rotating machinery, Mechanical Systems and Signal Processing 2013; 35: 108–126 C.
3 - Lacey SJ, An Overview of Bearing Vibration Analysis, Maintenance & asset management 2008; 23: 32-42.
4 - Symonds N, Corni I, Wood RJK, Wasenczuk A, Vincent D, Observing early stage rail axle bearing damage, Engineering Failure Analysis 2015; 56: 216-232.
5 - Zhao JS, Liu W, Zhanga Y, Feng ZJ, Ye J, Niu QB, Effects of gyroscopic moment on the damage of a tapered roller bearing. Mechanism and Machine Theory 2013; 69: 185–199.6 - Symonds N, Rolling contact fatigue - review and case study. In: Control and Reduction of Wear in Military Platforms NATO RTO-AVT-109, Williamsburg, USA, 7 - 11 Jun 2004.
7 - Rosado L, Forster NH, Thompson KL, Cooke JK, Rolling Contact Fatigue Life and Spall Propagation of AISI M50, M50NiL, and AISI 52100, Part I: Experimental Results. Tribology Transactions 2010; 53: 29-41.
8 - Arakere NK, Branch N, Levesque G, Svendsen V, Forster NH, Rolling Contact Fatigue Life and Spall Propagation of AISI M50, M50NiL, and AISI 52100, Part II: Stress Modeling. Tribology Transactions 2009; 53: 42-51
9 - Forster NH, Rosado L, Ogden WP, Trivedi HT, Rolling Contact Fatigue Life and Spall Propagation Characteristics of AISI M50, M50 NiL, and AISI 52100, Part III: Metallurgical Examination. Tribology Transactions 2010; 53: 52-59.
10 - El-Thalji I, Jantunen E, A descriptive model of wear evolution in rolling bearings, Engineering Failure Analysis 2014; 45: 204–224.
11 - Tsukahara H, Aime W, Burle A, Chavance D, Mouille E, Innovative application of Acoustic Bearing Condition Monitoring in High Speed Train Depots, In: 10th World Congress on Railway Research (WCRR) Sydney, Australia, 25-28 November 2013.
12 - Entezami M, Stewart E, Tutcher J, Driscoll W, Ellis R, Yeo G, Zhang Z, Roberts C, Kono T, Bayram S, Acoustic Analysis Techniques for Condition Monitoring of Roller Bearings. In: 6th IET Conference on Railway Condition Monitoring (RCM 2014), Birmingham, UK, 17-18 September 2014.
13 – Amini A, Entezami M, Huang Z, Rowshandel H and Papaelias M, Wayside detection of faults in railway axle bearings using time spectral kurtosis analysis on high-frequency acoustic emission signals, Advances in Mechanical Engineering 2016; 8: 1–9.
14 -M. Papaelias, Z. Huang, A. Amini, P. Vallely, N. Day, R. Sharma, Y. Kerkyras and S. Kerkyras, Advanced wayside condition monitoring of rolling stock wheelsets, In the Proceedings of The 11th ECNDT, 2014, Prague, Czech Republic, June 2014.
15 - Papaelias M, Amini A, Huang Z, Vallely P, Cardoso Dias D, Kerkyras S, Online condition monitoring of rolling stock wheels and axle bearings, J Rail and Rapid Transit 2016, 230: 709–723.
16 – Amini A, Entezami M, Papaelias M, Onboard detection of railway axle bearing defects using envelope analysis of high frequency acoustic emission signals. Case Studies In Non destructive Testing and Evaluation, 2016, 6: 8–16.

17 - Kalay S, French P, Tournay H, The safety impact of wagon health monitoring in North America. In: 9th World Congress of Railway research, Lille, France, 22-26 May 2011.
18 - SKF, Railway technical handbook Volume 2, Drive systems: traction motor and gearbox bearings, sensors, condition monitoring and services. PUB 42/P7 13085 EN, September 2012, ISBN 978-91-978966-6-5.
19 - SKF Axletronic sensors for the railway industry, PUB 42/P2 11007 EN, September 2010.
20 - Müller L, Sunder R, Innovative Condition Monitoring for Safety Related Bogie Components, In: 10th World Congress on Railway Research, Sydney, Australia, 25-28 November 2013.
21 - Bellaj S, Pouzet A, Mellet C, Vionnet R, Chavance D, Vibroacoustic measurement for bearing fault detection on high speed trains. In: 9th World Congress of Railway research, Lille, France, 22-26 May 2011.
22 – Vale C, Bonifacio C, Seabra J, Calçada R, Mazzino N, Massara E, Terribile S, Anguita D, Fumeo E, Saborido C, Vanhonacker T, De Donder E, Laeremans M, Vermeulen F, Grimes D, Novel efficient technologies in Europe for axle bearing condition monitoring – the MAXBE project, Transportation Research Procedia 2016, 14: 635 – 644.
23 - SKF: Bearing designs, tapered roller bearing units. Extract from the Railway technical handbook, volume 1, pp. 76-87.